

# Thiol-Click Based Polyglycerol Hydrogels as Biosensing Platform with In Situ Encapsulated Streptavidin Probes

Boonya Thongrom, Mathias Dimde, Uwe Schedler,\* and Rainer Haag\*

An in situ streptavidin-encapsulated hydrogel based on dendritic polyglycerol (dPG) which is functionalized with either an acrylate, allyl or acrylamide group and dithiolated polyethylene glycol (PEG) is constructed via a thiol-click chemistry approach and is investigated for biosensing applications. The hydrogel platform is screened for the encapsulation and release efficiencies of the model protein streptavidin under varying physicochemical conditions, for example, crosslinking chemistry reactions, the molar ratio between the two gel components, macromonomer concentrations or pH-values. By that, tailor-made hydrogels can be developed, which are able to encapsulate or release the model protein for several days based on its modality. Furthermore, the accessible binding site of encapsulated streptavidin or in other words, the biotin-binding performance is quantified, and the stability of the various hydrogel types is studied by rheology measurements, <sup>1</sup>H NMR, gel permeation chromatography (GPC), and mass loss experiments.

for diverse assays. However, streptavidin when fluorescently labeled is also used on the detection side of biosensors. The high sensitivity and stability of streptavidin-based biosensors enable both kinetic and quantification experiments.

In the field of immunoassays, streptavidin is also used both as a capture molecule for biotinylated species and as a detector molecule in sandwich assays.<sup>[6]</sup> Streptavidin-coated microtiter plates or beads allow an immobilization of any biotinylated molecule and thus provide flexibility for the solid phase assays compared to the antibody- or antigen-coated solid phase.<sup>[7]</sup> Streptavidin-coated materials, for example, glass slide,<sup>[2]</sup> silicon wafer,<sup>[2,8]</sup> gold-coated surface,<sup>[9,10]</sup> magnetic particle,<sup>[11]</sup> Teflon<sup>[12]</sup> or polymeric nanocarrier<sup>[13]</sup> are widely used in clinical

## 1. Introduction

Streptavidin is a homo-tetramer-type protein with a weight of roughly 55 kDa comprised of 4 binding sites.<sup>[1,2]</sup> It has been used as a biomolecular probe to sense or detect biotin since it binds strongly and specifically to streptavidin. The binding interaction between them is recognized as one of a strongest non-covalent interaction in nature so far.<sup>[3–5]</sup> Many modern biosensors exploit the high-affinity streptavidin-biotin interaction and thus provide access to a variety of assays based on it. Biomolecules, including proteins and nucleic acids, can be biotinylated using established protocols and immobilized on a streptavidin biosensor surface

diagnostics and there are numbers of manufacturers. However, there is still a sensitivity limit of detection for biotinylated compounds due to the limited streptavidin loading on the surface, its poor accessibility, and the low stability of immobilized streptavidin.


To improve its sensitivity for biotin detection, a 3D surface coating such as a polymeric brush<sup>[14,15]</sup> or hydrogels has been developed to cage it inside the 3D matrix.<sup>[1,2,16]</sup> Herrmann et al. have previously demonstrated the improvement of the sensitivity of biotin detection, compared to a commercially available streptavidin slides, by using an in situ streptavidin-immobilized hydrogel as a 3D sensing platform.<sup>[2]</sup> By using a hydrogel, the loading of streptavidin, and stability and accessibility of its binding site can be improved due to a water-based nature of the hydrogel, its high permeability inside the 3D network and its biocompatible gel material which can mimic the naturally environmental condition.

The use of immobilized streptavidin as a bioactive sensor on a coated surface has been extensively studied. Besides the quantification of the binding site,<sup>[2,17,18]</sup> the immobilized efficiency, or in other words an encapsulation efficiency in case of a streptavidin encapsulated inside a 3D matrix has been measured and is an essential factor for the validation of the material. This parameter can identify a streptavidin amount loaded inside and later imply directly the sensitivity of the detection. However, no systematic studies on the quantification of an encapsulation efficiency have been reported.

Click chemistry, a reaction which has high specificity, quantitative yield, benign condition and produces no or nontoxic

B. Thongrom, M. Dimde, R. Haag  
 Institut für Chemie und Biochemie  
 Freie Universität Berlin  
 Takustraße 3, 14195 Berlin, Germany  
 E-mail: haag@zedat.fu-berlin.de

U. Schedler  
 PolyAn GmbH  
 Schkopauer Ring 6, 12681 Berlin, Germany  
 E-mail: u.schedler@poly-an.de

 The ORCID identification number(s) for the author(s) of this article can be found under <https://doi.org/10.1002/macp.202200271>

© 2022 The Authors. Macromolecular Chemistry and Physics published by Wiley-VCH GmbH. This is an open access article under the terms of the Creative Commons Attribution-NonCommercial License, which permits use, distribution and reproduction in any medium, provided the original work is properly cited and is not used for commercial purposes.

DOI: 10.1002/macp.202200271

byproducts which can be easily removed without chromatographic technique, can be applied to a hydrogel crosslinking chemistry. Our group has used strain-promoted azide alkyne click (SPAAC) which is fast and bioorthogonal for the construction of a gel network.<sup>[2,19–21]</sup> However, the process to obtain its function on a gel precursor, especially cyclooctyne moiety is very costly and needs many synthetic and purification steps. Inverse electron demand Diels Alder reaction (iEDDA) is also of interest due to its even better bioorthogonality than strain-promoted azide alkyne click (SPAAC). A byproduct N<sub>2</sub> gas releasing inside the gel matrix might nevertheless interfere some optical analysis and not suitable for isolated space application.<sup>[22,23]</sup> To tackle these problems, a thiol-click chemistry crosslinking approach is proposed. Here, a high reaction specificity, a quantitative reaction, and easy purification step with high yields in terms of the synthesis of the gel precursors and remarkably good cost-effectiveness are given. The reaction between a thiol and a double bond acceptor is also fast and produces no byproduct.<sup>[24–27]</sup>

In this study, we introduce a hydrogel constructed by dendritic polyglycerol (dPG) and polyethylene glycol (PEG) building blocks via thiol-click reaction as a sensing platform to detect a biotin. Streptavidin is noncovalently encapsulated in situ during gel formation and its stability in different crosslink types of the hydrogel was analyzed.

## 2. Results and Discussion

### 2.1. Synthesis and Characterization of the Macromonomers for Hydrogel Preparation

The hydrogels developed in this study were based on multivalent dendritic polyglycerol (dPG), and polyethylene glycol (PEG) as a linear bifunctional crosslinker. To create a biocompatible 3D hydrogel network, dPG and PEG components were functionalized accordingly. For the crosslinking chemistry, thiol-Michael and a thiol-ene reaction were preferred due to their high yield, ease of preparation, high specification, straightforward, and inexpensive precursor preparation. For this purpose, a thiol group on a chain of the linear crosslinker PEG is linked to an olefinic acceptor group of the spherical dPG. The corresponding “thiol-click based” dPG-PEG hydrogels were investigated as a biosensing platform based on the concept of in situ encapsulation of a model protein streptavidin. The PEG dithiol crosslinker was synthesized according to the procedure from Mahadevegowda et al.<sup>[28]</sup> PEG(OH)<sub>2</sub> 1 was first mesylated at the chain end, then thiolated with thiourea and hydrolyzed. Two intact thiol groups were detected at the end chain of PEG-dithiol 3 by <sup>1</sup>H NMR (Figure S10, Supporting Information). A multivalent dPG hub 4 was functionalized with different functionalities to investigate the chemical and mechanical properties of the corresponding hydrogels. For this purpose, the multivalent hydroxyl groups of the dPG were functionalized with different olefinic acceptor groups for further crosslinking.

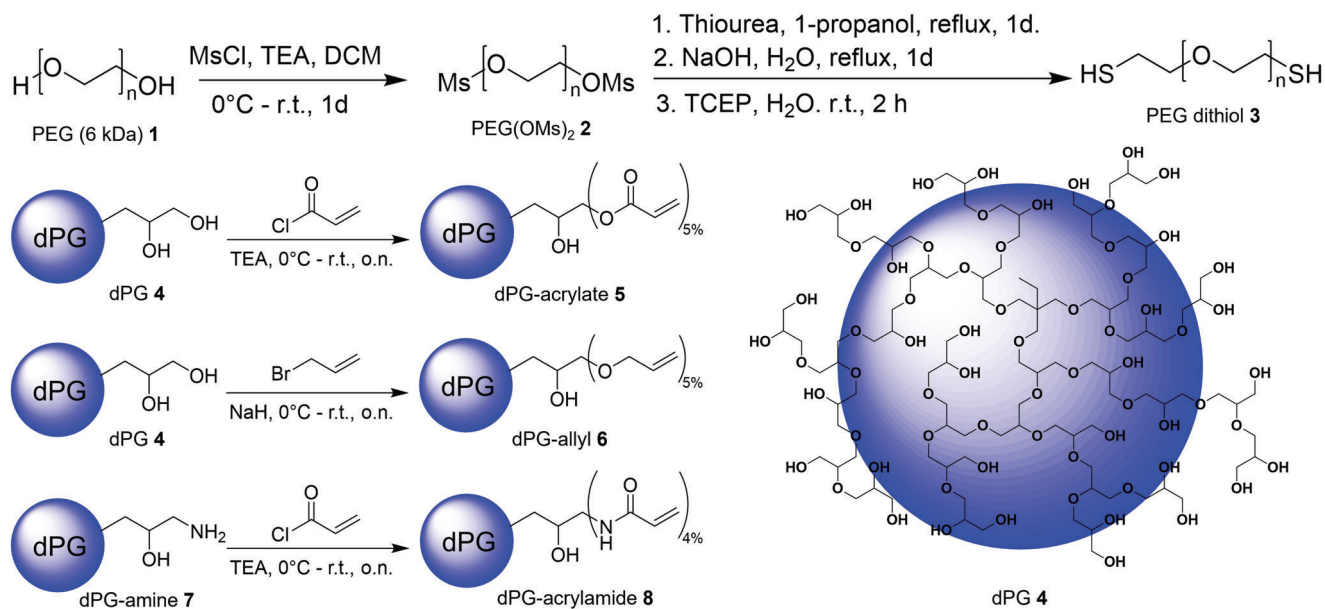
In the case of the dPG-acrylate 5, ≈5% functional groups were introduced by an acrylation reaction and characterized by <sup>1</sup>H NMR end group analysis (Figure S12, Supporting Information). The dPG-allyl 6 was prepared by allylation with allyl bromide, here 5% functional groups were introduced (Figure S12, Supporting Information). The dPG-acrylamide 8 was synthesized by an

acrylation reaction starting from dPG-amine (synthesized according to the procedure from Sebastian et al.<sup>[29]</sup>) whose number of amino groups were confirmed by <sup>1</sup>H NMR of dPG-NHBoc (Figures S13–S15, Supporting Information). A functionalization of 4% of acrylamide groups was calculated by <sup>1</sup>H NMR (Figure S16, Supporting Information). All reaction schemes of the individual gel components are shown in **Scheme 1**.

### 2.2. Hydrogel Formation and Flexibility Test

In this study, acrylate, allyl or acrylamide Michael acceptor groups on the dPG surface were used to verify their properties to form tailor-made hydrogels in terms of gel stability, flexibility and degradability. Furthermore, acrylate- and acrylamide-based hydrogels can be formed with PEG-dithiol by mixing both precursors, whereas allyl-based hydrogel formations need to be initiated via additional photo initiators and UV light. For the latter one, time-dependent start points, and defined reaction times favor the application in tissue engineering<sup>[30]</sup> and protein encapsulation.<sup>[31]</sup> All hydrogel samples in all experiments were measured in triplicate and each reported value is the mean value plus its standard deviation. Before investigating a biosensor application, the hydrogels with different crosslinking chemistry were rheologically characterized to determine the gel strength in terms of storage modulus (which directly refers to stiffness) and elasticity. Here, no biomolecule was yet added during gelation. A general procedure for the formation of thiol-acrylate hydrogel was to simply mix the 2 components (dPG-acrylate 5 and PEG-dithiol 3) under physiological pH. After successful crosslinking via thiol-Michael reaction, a solid hydrogel was formed. In case of thiol-allyl and thiol-acrylamide hydrogel preparations, a radical photoinitiator lithium phenyl-2,4,6-trimethylbenzoyl phosphinate (LAP) and UV light were required for a thiol-ene based reaction. After mixing the gel components (dPG-allyl 6 or dPG-acrylamide 8 with PEG-dithiol 3) with LAP, the mixing vessel was irradiated with monochromatic UV light of 365 nm for 10 min at the lateral side of a vessel. The UV light intensity was ≈190 μW cm<sup>-2</sup> (**Figure 1**). Moreover, the gelation of pure dPG-acrylate 5, pure dPG-allyl 6, and pure dPG-acrylamide 8 were studied in a similar approach to thiol-allyl and thiol-acrylamide gelation. The solution of pure dPG-allyl 6 was, however, unable to turn to a rigid hydrogel. The reason is probably that the side reaction of chain transfer to another allylic group inhibits the bond formation between two allylic groups.<sup>[32–34]</sup> On the other hand, the new bond formation on thiol-acrylamide hydrogel could come from both thioether bond (major) and C–C bond between the two double bonds (minor).<sup>[35,36]</sup>

In the gelation study, thiol-acrylate gel types were used because they are easy to prepare, and no catalyst or initiator was needed. Gelation screening based on the molar ratio of PEG to dPG component (PEG:dPG) was performed under similar conditions and the invert test tube method, in which the vessel of the gel mixture is inverted after the reaction time elapsed to see whether the mixture flows or not, was used to determine the gelation point. At higher ratio of dPG, there was no gel forming while starting from 1:1 ratio to higher PEG ratio, rigid gel emerges (Table S1, Supporting Information). Increasing the PEG ratio helps to build a 3D network structure and to form a solid hydrogel.



**Scheme 1.** Synthetic route for the functionalization of PEG-dithiol 3, dPG-acrylate 5, dPG-allyl 6, and dPG-acrylamide 8 and an idealized fragment structure of dendritic polyglycerol (dPG) 4.

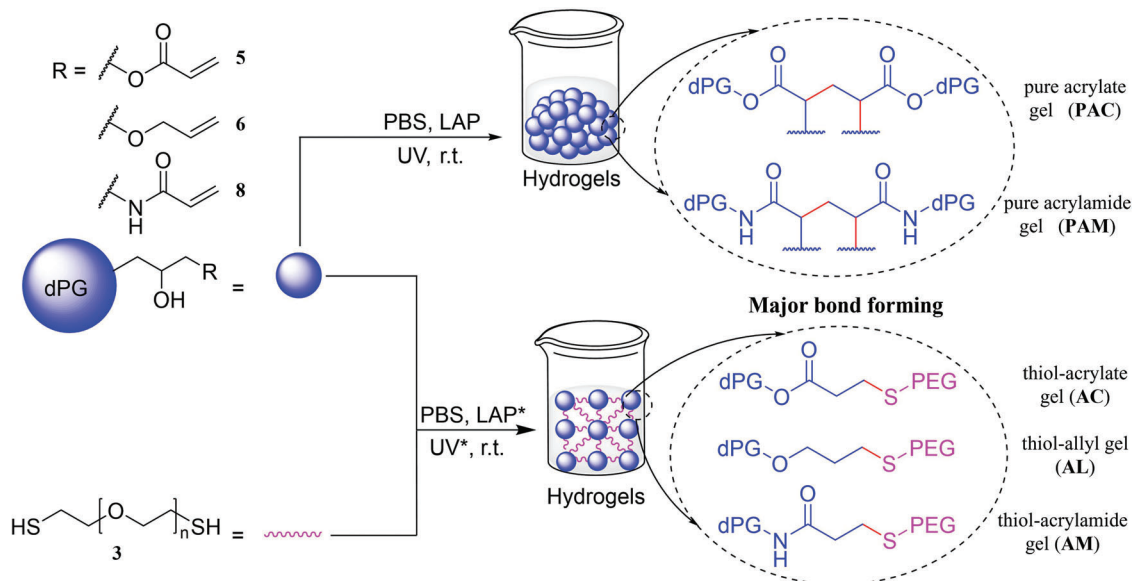


**Figure 1.** Hydrogel formation procedure of thiol-acrylate, thiol-allyl, thiol-acrylamide, pure acrylate, and pure acrylamide hydrogels. (\*) LAP and UV light were applied only to thiol-allyl and thiol-acrylamide gelation types.

The flexibility of each hydrogel type was determined using a rheometer with an 8 mm parallel plate geometry. The oscillation frequency sweep test at a constant strain of 1% and 25 °C was used to measure the storage modulus, which directly reflects the stiffness of a hydrogel. Thiol-acrylate hydrogels were prepared at different ratio and concentrations with designation as AC1, AC2, AC3 and AC4 while thiol-allyl gel AL1, thiol-acrylamide gel AM1, pure acrylate gel PAC1 and pure acrylamide gel PAM1 were prepared with additional LAP and UV light as given in detail in Table S2, Supporting Information. The result of the storage modulus

of each gel is shown in **Figure 2a**. As expected, the storage modulus increases when increasing the concentration and the ratio of PEG crosslinker as it increases the density of crosslink network, resulting in stiffer gel. However, when increasing PEG while decreasing dPG ratios in order to keep the same concentration as AC3, the storage modulus significantly decreases since lowering dPG component can lower the crosslink density.

The fracture point test of each hydrogel sample type at a gel concentration of 20% (AC2, AL1, AM1, PAC1, and PAM1) was determined by an oscillating amplitude sweep test in the range of

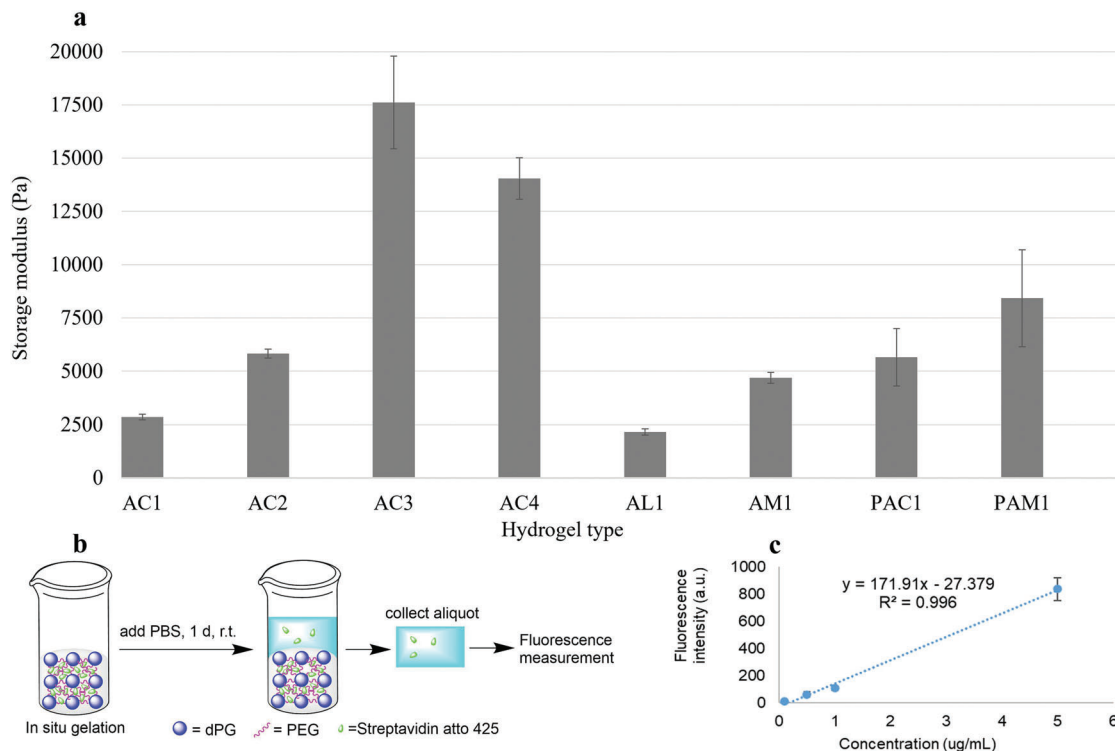


**Figure 2.** Characterization of hydrogels. a) Rheological measurements of the storage moduli of each hydrogel sample. b) Schematic procedure of the encapsulation efficiency test of a hydrogel after gelation in the presence of fluorescence-labeled streptavidin. c) Standard calibration curve of fluorescence-labeled streptavidin characterized by fluorescence measurements.

1–200% strain. This test can be used to preliminarily determine whether a hydrogel is elastic or brittle. The test measured the transition (crossover) point between storage modulus and loss modulus, where the storage modulus begins to decrease, and the loss modulus starts to increase. At this point, fracture or deformation cracking occurs at the macromolecular level. The results of the test are shown in Table S3, Supporting Information. PAC1 and PAM1 have low fracture value which indicates a brittle-type material while the remaining types (AC2, AL1, and AM1) are relatively elastic with high fracture point. These results explain that a solid hydrogel formed from a PEG crosslinker can impart elastic properties to a network structure due to its flexible linear chain. However, a hydrogel formed from only a dendritic and thus globular dPG component, despite its high storage modulus, can easily become brittle due to its hyperbranched structure.

### 2.3. Hydrogel Characterization and Determination of Encapsulation Efficiency

The model protein streptavidin was used for a proof-of-concept study to investigate the ability of the different hydrogel types which are usable for biosensing applications. Here, the hydrogel formation was tested and characterized by the usage of labeled streptavidin. The fluorescence-labeled streptavidin by Atto 425, a moderately hydrophilic coumarin-based structure with 90% quantum yield and excitation and emission maxima of 436 and 484 nm, respectively, was used for this study. The encapsulation efficiency of a hydrogel could be measured by quantify-

ing the fluorescence intensity of the fluorescent probe. To determine the encapsulation efficiency, a hydrogel with encapsulated fluorescence-labeled streptavidin was incubated overnight with phosphate buffer saline (PBS). The next day, the PBS aliquot on the gel was collected and measured with a fluorescence spectrometer to determine the corresponding intensity (Figure 2b). The detected intensity was calculated using the equation from the standard calibration curve of fluorescence-labeled streptavidin (Figure 2c) to determine the streptavidin concentration, which was later converted to its weight ( $\mu\text{g}$ ). Once the weight in an aliquot was known, the weight of fluorescence-labeled streptavidin remaining in the hydrogel could be calculated, to obtain the encapsulation efficiency. Factors such as the molar ratio of PEG:dPG, the pH of a mixture, the storage conditions of the PEG-dithiol stock solution, and the gel concentration were screened by using thiol-acrylate gel type to find an optimum for the loading capacity of fluorescence-labeled streptavidin.

First, the encapsulation efficiency was investigated as a function of the different molar ratios of PEG:dPG. The molar ratio of dPG was kept constant while the molar ratio of PEG was increased by 2:1 (AC5), 3:1 (AC6), 5:1 (AC7), 7:1 (AC8), and 9:1 (AC9) of PEG:dPG and 3  $\mu\text{g}$  of streptavidin was added in situ to each replicate sample (see Table 1). The encapsulation efficiency results are shown in Figure 3a. The AC5 sample exhibits the highest encapsulation efficiency of  $\approx 70\%$ , and the efficiency decreases with increasing PEG ratio. We assumed that the higher the hydrophilic PEG content, the stronger the swelling of the hydrogel occurs, resulting in network loosening and a higher leaching of streptavidin into the PBS aliquot. This assumption

**Table 1.** Preparation of different gel types with in situ encapsulation of fluorescence-labeled streptavidin for the determination of encapsulation efficiency from different stock solution of precursors (45% w/v PEG-dithiol 3, 37.6% w/v dPG-acrylate 5, 42.3% w/v dPG-allyl 6, 26.4% w/v dPG-acrylamide 8, 5 mg mL<sup>-1</sup> LAP). The volume of fluorescence-labeled streptavidin (1 mg mL<sup>-1</sup>) were added 3  $\mu$ L in all gel samples which were prepared at the total volume of 38  $\mu$ L. Thiol-acrylate (AC), thiol-allyl (AL), thiol-acrylamide (AM), pure acrylate (PAC), and pure acrylamide (PAM).

Gel code	PEG		dPG		LAP	PBS	Mole ratio	Mole ratio	Conc. [%w/v]
	Volume [ $\mu$ L]	Mole [ $\mu$ mol]	Volume [ $\mu$ L]	Mole [ $\mu$ mol]	Volume [ $\mu$ L]	Volume [ $\mu$ L]	SH:ene	PEG:dPG	
AC5	6.5	0.49	6.4	0.24	-	22.1	4:6	2:1	14
AC6	9.7	0.73	6.4	0.24	-	18.9	6:6	3:1	18
AC7	16.1	1.21	6.4	0.24	-	12.5	10:6	5:1	25
AC8	22.5	1.69	6.4	0.24	-	6.1	14:6	7:1	33
AC9	28.6	2.14	6.4	0.24	-	0	18:6	9:1	40
AC10	4.7	0.35	4.6	0.17	-	25.7	4:6	2:1	10
AC11	9.3	0.7	9.2	0.34	-	16.5	4:6	2:1	20
AC12	14	1.05	13.6	0.51	-	7.4	4:6	2:1	30
AC13	16.3	1.22	15.9	0.6	-	2.8	4:6	2:1	35
AL2*	9.3	0.7	8.1	0.34	4.2	13.4	4:6	2:1	20
AM2*	9.3	0.7	13	0.34	4.2	8.5	4:5	2:1	20
PAC2*	-	-	20.3	0.76	4.5	10.2	-	-	20
PAM2*	-	-	28.9	0.76	4.5	1.6	-	-	20

\*These samples contain 10 mol% LAP (based on PEG 3) and are exposed to 10 min UV.

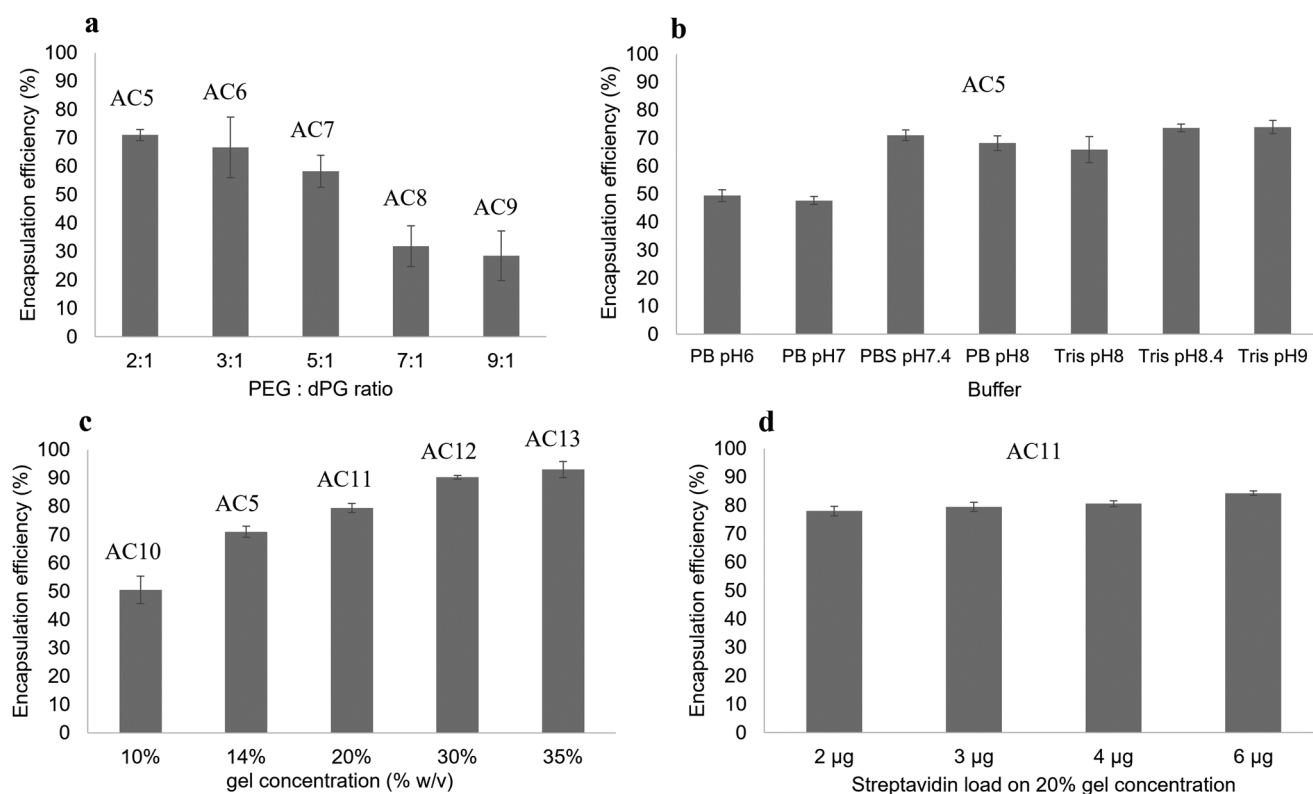


**Figure 3.** Screening of the encapsulation efficiency based on the variation of different parameters. a) Various molar ratios of PEG:dPG (2:1 [AC5], 3:1 [AC6], 5:1 [AC7], 7:1 [AC8], and 9:1 [AC9] ratio). b) Various biological buffers of gel type AC5. c) Gel concentrations (10% [AC10], 14% [AC5], 20% [AC11], 30% [AC12], and 35% w/v [AC13]). d) Loading of fluorescence-labeled streptavidin of 20% w/v gel concentration (AC11).



has been confirmed by the mass swelling ratio (Figure S1, Supporting Information) as the mass swelling ratio increases when increasing the molar ratio of PEG, resulting in enhancing hydrophilicity of the gel system to hold more water content inside a gel matrix. The lowest swelling value was identified from gel AC5 which has a low tendency to wrinkle, suitable for a confined space experiment (in this case, a 2 mL glass vial). This is because a well swelling hydrogel in a confined container expands dramatically in all directions after immersion in aqueous media, resulting in gel stresses, and eventually in wrinkling and cracking.<sup>[37,38]</sup>

Second, the encapsulation efficiency was studied based on the pH of a gel mixture and the state of the PEG-dithiol stock solution. The pH of hydrogel AC5 was varied from pH 6 to pH 9 using phosphate buffer (PB), PBS, and tris(hydroxymethyl)aminomethane (Tris) buffer solutions. Here, a higher pH of the mixture leads to higher encapsulation efficiency, as a more basic pH promotes thiolate formation,<sup>[39,40]</sup> that can react more efficiently with the double bond of an acrylate group,<sup>[41]</sup> leading to denser network formation and ultimately higher encapsulation efficiency (Figure 3b). The efficiency of the PBS pH 7.4 sample appears to be relatively high at 70% efficiency and comparable to those with higher pH values. Therefore, PBS pH 7.4 (physiological pH) solution was used to prepare hydrogels in all follow-up experiments. Furthermore, the storage conditions of PEG-dithiol 3 were studied by gel AC5. In case of PEG stock solution, the efficiency of a two-month-old PEG-dithiol solution stored in the refrigerator ( $\approx 4$  °C) was comparable to the one with a freshly prepared stock-solution (Figure S2, Supporting Information). The encapsulation efficiency results from both stock solutions showed comparable result, suggesting that a PEG stock solution can be stored for at least two months.

Third, the encapsulation efficiency depended on the hydrogel concentration was conducted. Hydrogels ranging from 10% (AC10), 14% (AC5), 20% (AC11), 30% (AC12) to 35% w/v (AC13) were prepared. The result of the encapsulation efficiency is shown in Figure 3c. As expected, a hydrogel with the highest molar ratio (AC13) shows the highest efficiency as the higher concentration leads to higher crosslink density, thereby entrapping streptavidin in a better way. Gel AC12 and AC13 show comparable results of encapsulation efficiency, but AC10 and AC11 show a gap difference in encapsulation efficiency of almost 30%. Therefore, it is of interest to screen samples at 10% (AC10), 20% (AC11), and 30% w/v (AC12) gel concentrations and calculating their loading capacity factor.

Finally, the encapsulation efficiency was investigated as a function of loading with fluorescence-labeled streptavidin. The labeled Streptavidin was loaded in situ in varying amounts into a hydrogel with concentration of 10% (AC10), 20% (AC11), and 30% w/v (AC12) gel. The results of all gel concentrations show that the efficiency typically increases with an increasing streptavidin loading. However, Gel AC11 and AC12 showed no significant differences in the efficiency (Figures S3 and S4, Supporting Information). From an economic point of view, AC11 with 3  $\mu$ g streptavidin loading would be a good candidate for further application studies, as it shows comparably high encapsulation efficiency at comparatively low material cost. Furthermore, no gel stress (wrinkle) was spotted for AC11.

In the cases of thiol-allyl and thiol-acrylamide gel types, The LAP photoinitiator, and UV light at a wavelength of 365 nm are

required.<sup>[42–44]</sup> Both AL2 and AM2 hydrogels were tested by two main parameters: the amount of LAP and a UV exposure time. At first, the determination of the stability limit of Atto 425 dye must be performed since a typical fluorescence dye can get exhausted by a long UV exposure time. The resulting intensity of even after 20 min exposure shows no significant difference compared to the non-treated control (Figure S5, Supporting Information).

The encapsulation efficiency based on thiol-allyl gel (AL2) was investigated by studying the effect of a UV irradiation time while LAP amount was kept constant. Gel AL2 was exposed to UV light at different time periods from 5 to 20 min. The resulting encapsulation efficiency of a sample at a 10 min exposure seems to be sufficient to achieve high efficiency comparable to the ones with higher exposure times (Figure 4a). Besides that, the encapsulation efficiency based on various amount of LAP photo initiator was investigated. Gel AL2 was prepared by different amounts of LAP from 1 to 20 mol% at 10 min UV irradiation. Here, the sample with 10 mol% LAP has a relatively high encapsulation efficiency ( $\approx 80\%$ ) compared to the samples with 15 mol% and 20 mol% LAP ( $\approx 70\%$ ) (Figure 4b). However, the sample with 1 mol% LAP did not form a solid hydrogel in the experimental time frame.

Furthermore, encapsulation efficiency studies based on a thiol-acrylamide type hydrogel (AM2) were investigated. Beginning with the various exposure times which were applied to gel AM2 with slightly modified procedure, the 3 samples were incubated with PBS immediately after UV exposure at minute 1, 10, and 20 respectively, while another sample with 10 min exposure was kept at room temperature in the dark overnight before incubation. Interestingly, the encapsulation efficiency of the latter one improved, compared to the one at the same exposure but without a pause, while the others (without a pause) show increased efficiencies with elevated exposure times (Figure 4c). This is because a thiol-acrylamide reaction undergoes not only radical reaction but also addition reaction catalyzed by weak basic condition (pH7.4) as the Michael acceptor is electrophilic enough to be attacked by thiolate group of PEG-dithiol, resulting in the higher crosslink network and the higher efficiency.<sup>[41,45,46]</sup> Next, the encapsulation efficiency based on different amounts of LAP from 0.1 mol% to 20 mol% was studied at constant exposure time. Unlike thiol-allyl gel type which suffers from chain transfer side reactions,<sup>[32–34]</sup> thiol-acrylamide gel could form a rigid gel starting from 0.1 mol% LAP (Figure 4d). As expected, increasing amounts of LAP helps to improve the encapsulation efficiency and at 10 mol% LAP, a maximum is reached at 70%. In summary, 10 mol% LAP and a 10 min UV irradiation time are the best conditions to generate the hydrogels of pure acrylate (PAC2) and acrylamide (PAM2) among the screened parameters.

Despite their hard and brittle property, pure acrylate- (PAC2) and acrylamide- (PAM2) type hydrogels were investigated with respect to their encapsulation efficiency. The result shows that the two types of gels have comparable encapsulation efficiencies of 65–70% (Figure S6, Supporting Information).

#### 2.4. Quantification of Accessible Binding Site of Streptavidin

The most important function of the streptavidin surfaces is the specific binding of biotin or biotinylated compounds. This has

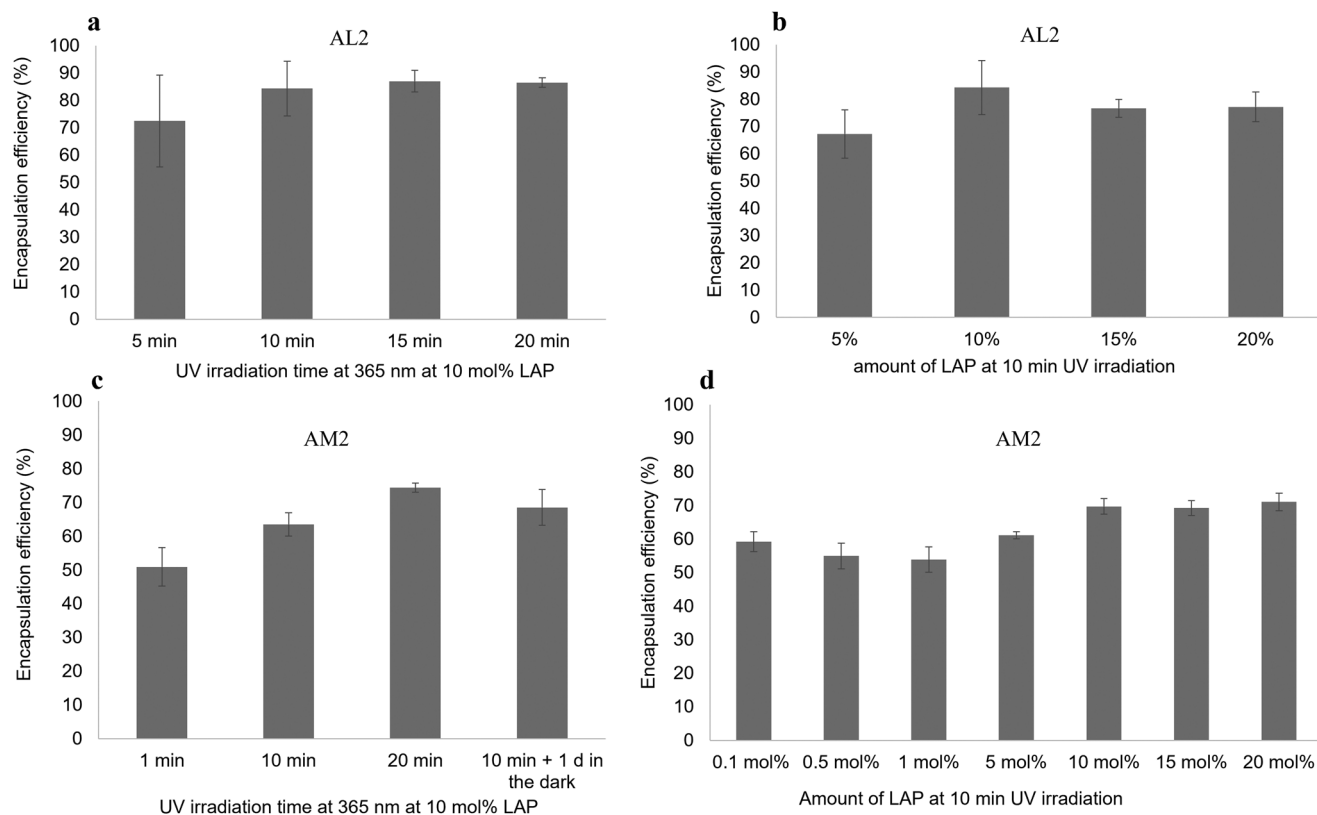


**Figure 4.** Screening of the encapsulation efficiency of AL2 and AM2 gels at different conditions: a) the encapsulation efficiency result of AL2 based on different UV exposure times at 365 nm; b) the encapsulation efficiency of 20% w/v thiol-allyl hydrogel at 10 min UV exposure time based on different amounts of LAP photo initiator; c) the encapsulation efficiency of AM2 gel on different UV exposure times at 365 nm; and d) the encapsulation efficiency of AM2 at 10 min UV exposure time based on different amounts of LAP photo initiator.

been done not only in biosensing to detect the biotinylated compounds, but has also been used to enrich or separate these compounds. Streptavidin has 4 binding sites for biotin, and the sensitivity to biotin could be reduced by blocked or inaccessible binding pocket. Therefore, it is crucial to demonstrate not only the encapsulation efficiency but also the structural integrity as well as accessibility of the binding sites to realize biosensing applications with biotin. For all hydrogel types described above (thiol-acrylate, thiol-allyl, thiol-acrylamide, pure acrylate, and pure acrylamide), the accessible binding sites of streptavidin encapsulated in situ in a hydrogel matrix were determined. To quantify the accessible binding sites, the colorimetric HABA-streptavidin complex was used. HABA (4'-hydroxyazobenzene-2-carboxylic acid) is a dye molecule that has a much lower binding constant to streptavidin than biotin and thus can bind only moderately to the binding site of a streptavidin. The HABA-streptavidin complex shows an absorption maximum at 500 nm, while HABA alone shows an absorption maximum at 350 nm. When biotin is added to a solution of a HABA-streptavidin complex, biotin completely replaces HABA due to the strong binding affinity of streptavidin-biotin, which is superior to that of a HABA-streptavidin complex, resulting in a decrease in the absorption signal at 500 nm. In this experiment, the assay was divided into two parts. The first part was to quantify the binding sites with HABA (HABA assay), and the second part was to quantify the binding sites of the HABA-streptavidin complex with biotin (biotin assay).

In this method, a pure, non-fluorescently labeled streptavidin was encapsulated in situ in a hydrogel matrix (Table S2, Supporting Information). The hydrogel was treated with an excess of HABA solution, incubated overnight, and light absorption was then measured at 500 nm. The positive control was prepared by mixing a streptavidin and HABA solution with the same amount applied to the hydrogel samples. The resulting absorption of all types of hydrogel samples was compared to the value of the positive control, which was set as 4 intact binding sites to obtain the number of accessible binding sites. The result shows that the encapsulated streptavidin has an average of above 3 accessible binding sites as well as high binding capacity in all types of hydrogels (Table 2). This means that most of the binding sites of the encapsulated streptavidin are retained and thus accessible for binding with biotin.

Furthermore, quantification of the accessible binding site of encapsulated streptavidin by biotin was performed. In this way, instead of loading streptavidin into a hydrogel, the streptavidin-HABA complex was loaded. Then, an excess of biotin was added and incubated. The control was prepared by mixing HABA and biotin (same amount applied to the hydrogel samples) in the PBS solution. The absorbance was determined at 350 nm as a positive control, fixed at 4 binding sites, since theoretically all HABA molecules can be substituted by biotin and released into the solution. The negative control was performed at a wavelength of 500 nm assuming that no streptavidin-HABA complex

**Table 2.** Number of accessible binding sites of in situ encapsulated streptavidin in all types of hydrogels, tested by HABA/biotin assay.

Hydrogel type	Accessible binding sites of encapsulated streptavidin					
	By HABA test			By biotin test		
	No. of Binding sites	SD	Binding capacity (microgram biotin/milliliter gel)	No. of Binding sites	SD	Binding capacity (microgram biotin/milliliter gel)
Thiol-acrylate	3.5	0.1	20.5	4.0	0.1	23.4
Thiol-allyl	3.4	0.1	19.9	3.1	0.1	18.2
Thiol-acrylamide	3.7	0.5	21.6	3.4	0.1	19.9
Pure acrylate	3.2	0.3	18.7	3.0	0.1	17.6
Pure acrylamide	3.1	0.1	18.2	3.1	0.1	18.2

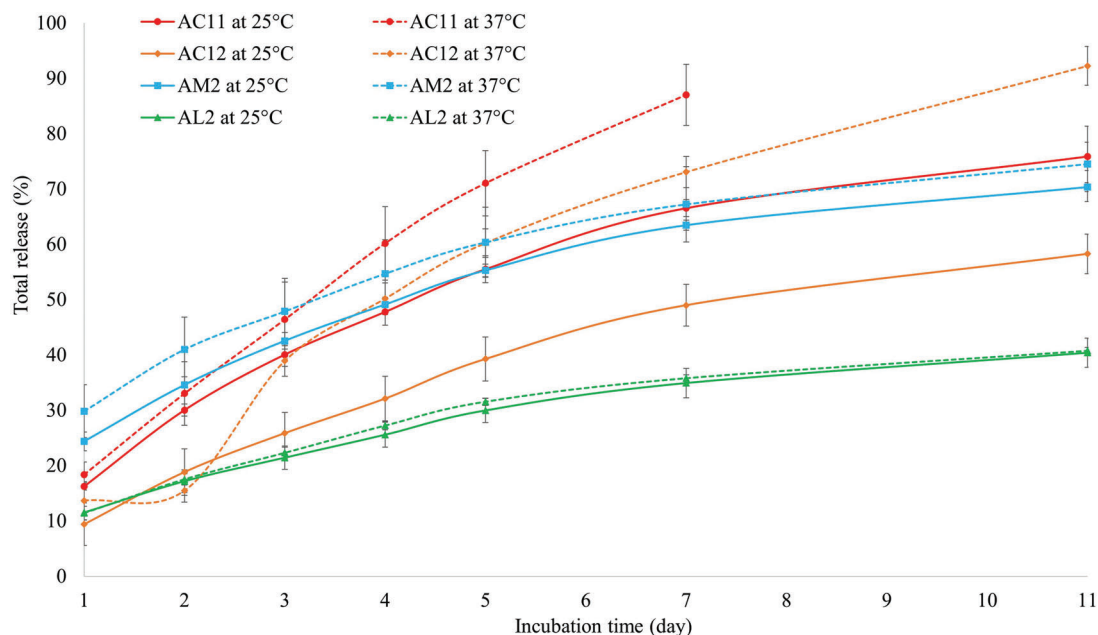


**Figure 5.** Release study of the in situ encapsulated fluorescence-labeled streptavidin in thiol-acrylate (AC11 and AC12), thiol-allyl (AL2), and thiol-acrylamide (AM2) hydrogels.

remained. The resulting binding sites and binding capacity are relatively similar to the previous experiment (Table 1). It can be concluded that in situ encapsulated-streptavidin hydrogel with different crosslinking chemistry types can retain most of the accessible binding sites (above 3 on average) of streptavidin as well as the binding capacity and can serve as an effective sensing platform for biotin and biotinylated species.

## 2.5. Kinetic Release Study and Degradation-Stability Test

To broaden the application horizon of this “thiol-click” hydrogel platform, release and stability studies are of interest for many application areas,<sup>[47–51]</sup> where the controlled release of a biomolecule or a drug has been studied at different temperatures and with different types of hydrogel platforms. In this particular case, the focus was on the stability of the hydrogels. In our study, a fluorophore-labeled streptavidin (Atto 425), was encapsulated in

situ in the different hydrogel types, and the release of streptavidin was followed with by fluorescence intensity measurements, similar to the encapsulation efficiency measurement with slight modification. The experiment was performed at 25 and 37 °C, and the incubation time was extended from day 1, 2, 3, 4, 5, 7 to 11. The release of non-covalently immobilized streptavidin was controlled by the macromolecular network (structure and density) of a hydrogel and by non-covalent interactions. Thiol-acrylate (AC11 and AC12), -allyl (AL2), and -acrylamide (AM2) gels were tested. The results show that all samples generally have a tendency to release streptavidin over a longer period of time, especially at a higher temperature in combination with the acrylate-based crosslinking (Figure 5). Interestingly, gel AC11 at 37 °C became apparently softened by time and turned to solution in the last day. The reason lies to an ester bond from acrylate group, which was cleaved by hydrolysis, accelerated by high temperature.<sup>[52,53]</sup> Unlike AC11, gel AC12 with higher crosslink density was rigid enough to resist degradation through the end of the test. Gel AL2, on the



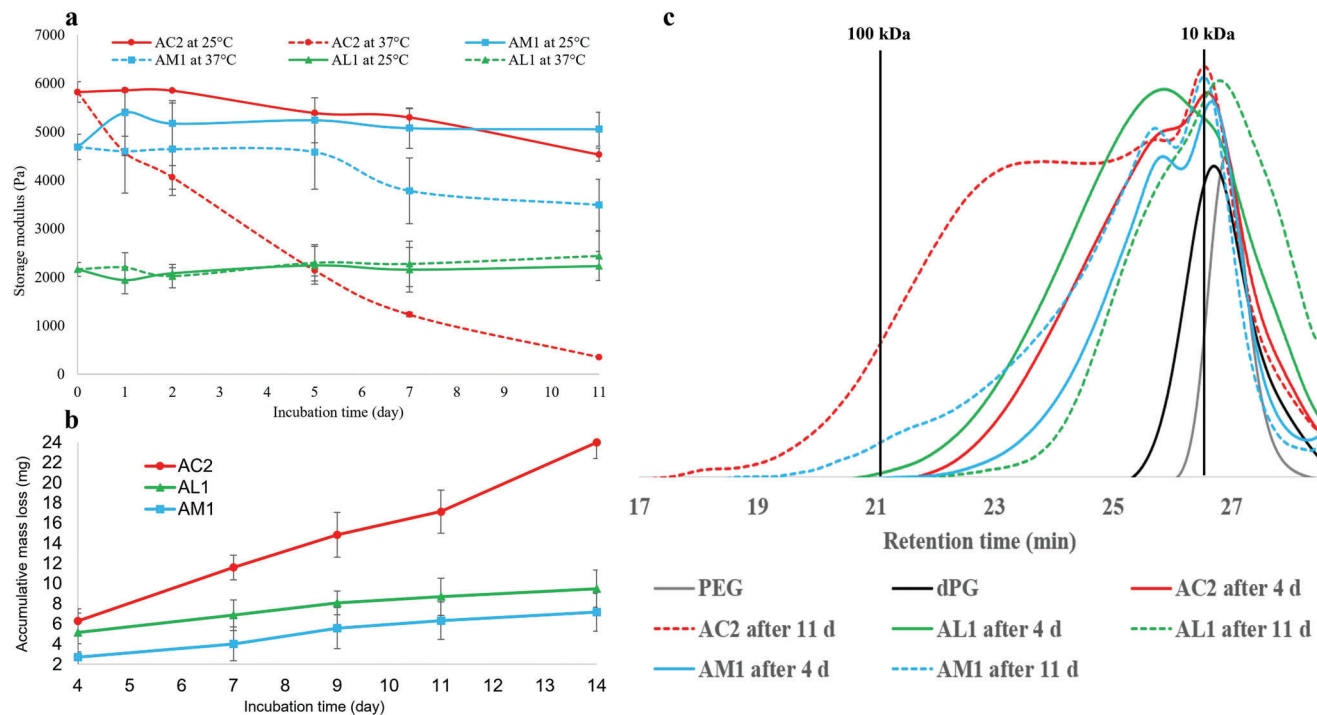


**Figure 6.** Degradation study of thiol-acrylate (AC2), -allyl (AL1), and -acrylamide (AM1) hydrogels. a) Rheological characterization by oscillatory frequency sweep test at 1% strain and storage modulus at 1 Hz. b) Accumulative mass loss at 37 °C. c) Normalized gel permeations chromatogram of the incubated hydrogel samples at day 4 and day 11 at 37 °C in comparison to the precursor PEG and dPG.

other hand, shows slowest release with less than 40% even after 11 days, despite the fact that it has the lowest storage modulus (Figure 2) (or biggest mesh size [Figure S7, Supporting Information]) among them. The reason could come from the London dispersion interaction<sup>[54]</sup> between the large hydrophobic surface of a streptavidin<sup>[55,56]</sup> and thiol-allyl crosslinking region which is also hydrophobic, resulting in stable immobilization of streptavidin and slower release. It should be noted that besides the physical network density, the chemistry of the functional groups also has a great influence on the release, as it can be basically degradable or non-degradable.

To analyze the impact of the crosslinking chemistry, a degradation study of acrylate (AC2), allyl (AL1) and acrylamide (AM1) functional groups was performed by 4 main characterization methods: mechanical test by rheology, <sup>1</sup>H NMR spectroscopy, mass loss compilation, and molecular weight analysis by gel permeations chromatography (GPC). Starting with mechanical characterization by rheology, the resulting data was picked at 1 Hz in oscillatory frequency sweep test. The decrease of the storage modulus of AC type is obvious and get drastically accelerated at higher temperature as it is shown the clear sign of degradation, while the other types remain steady (Figure 6a).

In addition, the accumulative mass loss of AC2, AL1 and AM1 gels was calculated, and an aliquot of the sample was characterized by <sup>1</sup>H NMR and GPC. In case of <sup>1</sup>H NMR analysis, the water in PBS buffer was replaced by deuterium oxide and this was used for this experiment at only 37 °C to distinguish the unequivocal degradation study. The NMR spectrum of Gel AC2 clearly shows a sign of the higher peak intensity of not only an unreacted acrylate double bond (which was left since less PEG dithiol ratio,

2:1, was used) in the 5.5–7 ppm range, but also the main polymer backbone peaks at 3–4 ppm as well as at the reaction point (the peak of 2.8–2.9 ppm) compared to the others in the longer period (Figure S8, Supporting Information). This probably indicates that a large amount of the gel substances dissolve in the aliquot part, suggesting a degradation product, unlike AL1 and AM1 gels which did not show a signal of degradation as can be seen from the lower peak intensities developed by time. Furthermore, the accumulative mass loss and the GPC results can support the assumption. Accumulative mass loss was measured by accumulatively measuring the dry weight of substance in aliquot part. From the result, the mass loss of AC2 increases noticeably while the ones from gels AL1 and AM1 increase insignificantly slowly (Figure 6b). The degradation product of gel AC2 is further evidenced by the normalized GPC data as seen from the large shoulder peak which appears at almost close to 100 kDa after 11 days (Figure 6c).

### 3. Conclusions

A scalable thiol-click based hydrogel was constructed by reacting 6 kDa PEG dithiol with 10 kDa dendritic polyglycerol, which was functionalized with 3 different functional groups: acrylate, allyl, or acrylamide. Besides hydrogel characterization studies in terms of gel stability, flexibility and degradability, in situ encapsulated-streptavidin hydrogels were analyzed regarding to their encapsulation efficiency under various physicochemical conditions. Here high efficiencies and high accessible binding sites and binding capacities of streptavidin were found for all gel types. Furthermore, the release study of in situ encapsulated-streptavidin gel

over several days was investigated. The encapsulated streptavidin from thiol-acrylate gel type leached out much faster than those from thiol-allyl and -acrylamide gels, due to ester-group degradation, which was experimentally proven by rheology measurements,  $^1\text{H}$  NMR, GPC and accumulative mass loss experiments.

In conclusion, all hydrogel types performed well as biosensing platforms. Differences in the hydrogel structure and thus in their properties could be used for different applications. Thiol-acrylate based gels have the highest encapsulation efficiency of streptavidin. However, due to their degradability, they are only feasible for biosensing applications with incubations and experimental times of less than 1 day. Acrylate containing hydrogels could further be used for applications requiring their ability to degrade such as wound healing<sup>[57]</sup> or cell encapsulation,<sup>[58]</sup> whereas a less or non-degradable alternative, radical-mediated thiol-allyl and thiol-acrylamide based hydrogels could be applied in tissue engineering<sup>[30]</sup> or bio-ink application<sup>[59]</sup> where a gel remains stable over a long period of time.

## 4. Experimental Section

**Materials:** All chemicals were purchased from Merck KGaA, Darmstadt, Germany and/or its affiliates and used without any further purification, unless otherwise stated. Diethyl ether (100%) was purchased from VWR chemicals. *N,N*-Dimethylformamide (DMF, 99.8%) was purchased from Acros Organics. Triphenylphosphine (99%) was purchased from Alfa Aesar. Sodium hydroxide (pellets), Sodium hydroxide (99.5%), dichloromethane (DCM, 99%) and ethyl acetate were purchased from Fischer Scientific. Micro fluorescence cuvette (ES-Quartz glass) with the optical path length of Optical path length  $10 \times 4$  mm was purchased from Portmann Instruments. UV bypass filter with 365 nm monochrome light and 49 mm diameter was purchased from Vision Light Tech B.V. The average weight molecular weight of 10 kDa of dPG was prepared as previously reported<sup>[60–62]</sup> with the improved method.<sup>[63]</sup>

**Instrumentals:** All NMR spectra ( $^1\text{H}$  and  $^{13}\text{C}$ ) were recorded at 300 K by on a Jeol Eclipse 500 MHz (Tokyo, Japan) or a Bruker AVANCE III 700 MHz spectrometer (Billerica, MA, USA). Chemical shifts  $\delta$  were reported in ppm and the deuterated solvent peak was used as a standard. The elemental assessment was performed by Vario EL CHNS element analyzer by Elementar Analysensysteme GmbH (Langensfeld, Germany). All GPC chromatograms were recorded in water with an Agilent 1100 equipped with an automatic injector, isopump, and Agilent 1100 differential refractometer (Agilent Technologies, Santa Clara, CA, USA). The PSS Suprema (precolumn), 1x with pore size of 30 Å, 2x with pore size of 1000 Å column, was calibrated against Pullulan standards prior to measurements. All fluorescence data were resulted from JASCO FP-6500 spectrometer. The absorbance of the quantification of streptavidin binding site was obtained from a microplate reader (TECAN infinite M200Pro).

**Rheology:** All the rheology data of hydrogel samples were characterized by Malvern Instruments Kinexus equipped with the parallel plate of 8 mm diameter and the average normal force of estimate 0.1 N at 25 °C. The data were analyzed by an oscillatory frequency sweep strain controlled test with 1% strain (which was obtained from a linear viscoelastic range of an amplitude sweep test) and the reported storage modulus ( $G'$ ) of a rigid hydrogel were picked at 1 Hz. The rupture point of a hydrogel was determined by oscillatory amplitude sweep test ranging from 1–200% strain at a constant 1 Hz.

**Functionalization of PEG(OMs)<sub>2</sub> 2:** PEG 1 (6 kDa, 20 g, 3.3 mmol, 1 equiv.) was first dried at 70 °C under vacuum overnight. The dried PEG was then purged with Argon gas and cooled down to room temperature and was dissolved in anhydrous DCM (100 mL). Triethylamine (TEA, 2.77 mL, 20 mmol, 6 equiv.) was added to the solution and the reaction flask was then cooled on ice bath. Methanesulfonyl chloride (1.03 mL, 13.3 mmol, 4 equiv.) was added dropwise to the solution and the reac-

tion then was stirred overnight. Afterward the ice bath was removed and the crude product was washed thrice with brine. The DCM layer was then dried with  $\text{Na}_2\text{SO}_4$  and concentrated on the rotary evaporator. The concentrated crude was then precipitated in cooled diethyl ether. After being dried overnight under vacuum, the precipitate product results in a white powder with 95% isolated yield.  $^1\text{H}$  NMR (500 MHz,  $\text{CDCl}_3$ ,  $\delta$  [ppm]): 3.07 (3H, s), 3.48–3.78 (m), 4.37 (2H, t) (Figure S9, Supporting Information).

**Functionalization of PEG Dithiol 3:** Dimesylated PEG 2 (PEG(OMs)<sub>2</sub>, 19 g, 3.2 mmol, 1 equiv.) was dissolved in 1-propanol (100 mL) and thiourea (1.02 g, 13.3 mmol, 4 equiv.) was then added to the solution. The solution was refluxed overnight to obtain diisothiuronium PEG intermediate. After 1-propanol was removed from the mixture, NaOH (0.53 g, 13.3 mmol, 4 equiv.) and water (100 mL) were added and the solution was then refluxed overnight. Afterward, tris(2-carboxyethyl)phosphine (TCEP, 1.67 g, 6.7 mmol, 2 equiv.) was added and the reaction was run for 2 h. The product was purified by first adding NaCl to the reaction mixture until saturated point, then extracting the product with DCM thrice and drying it with  $\text{Na}_2\text{SO}_4$ , concentrating the DCM layer and finally precipitating it in cooled diethyl ether. The precipitate was allowed to dry under vacuum overnight to later obtain PEG dithiol product 3 as a pale yellowish powder with an 88% isolated yield.  $^1\text{H}$  NMR (500 MHz,  $\text{CDCl}_3$ ,  $\delta$  [ppm]): 1.59 (1H, t), 2.69 (2H, quat), 3.48–3.78 (m). Elemental analysis; N 0.13; C 54.24; S 2.02; H 8.47 (Figure S10, Supporting Information).

**Functionalization of dPG Acrylate 5:** Dried dPG 4 (10 kDa (4.94 g, 0.49 mmol, 1 equiv.) was dissolved in DMF (50 mL). The reaction flask was then cooled with ice bath and TEA (0.88 mL, 6.42 mmol, 13 equiv.) was added to the solution. Acryloyl chloride (0.4 mL, 4.94 mmol, 10 equiv., aimed to have  $\approx 5\%$  acrylate functional groups on dPG) was added dropwise to the mixture and the reaction flask was allowed to stir overnight. Afterward, the mixture was concentrated and purified by dialysis by using 2 kDa cutoff benzoylated cellulose dialysis tube in water for 2 d. After the purification, the mixture was concentrated and stocked as an aqueous solution (80% isolated yield). The  $^1\text{H}$  NMR shows the peaks of double bond and the main backbone peak. The estimate calculation of a number of the functional groups relies on the comparison between the integral of the repeating unit peak which refers to five protons and the integral of the double bond peaks. As for the dPG acrylate 5, the authors assumed that one repeating unit glycidol contains one free hydroxy group. If 100% functionalization happens, it means one repeating unit (five protons) contains one proton peak of the double bond. Thus, the integral of 0.05 of a proton peak refers to 5% acrylate functional group. As aforementioned, one repeating unit glycidol ( $M_w$  74 g  $\text{mol}^{-1}$ ) contains one free OH group. So, in one polymer molecule ( $M_w$  10 000 g  $\text{mol}^{-1}$ ), there were 135 free OH groups by average estimation and dPG acrylate with a 5% functional group corresponding to roughly 6 groups of acrylates.  $^1\text{H}$  NMR (500 MHz,  $\text{D}_2\text{O}$ ,  $\delta$  (ppm)): 0.88 (3H, broad s, initiator backbone), 1.38 (2H, broad s, initiator backbone), 3.44–4.32 (m, backbone repeating units), 6.05 (1H, broad s), 6.26 (1H, broad s) and 6.50 (1H, broad s) (Figure S11, Supporting Information).

**Functionalization of dPG Allyl 6:** To a DMF (10 mL) solution of dried dPG 4 (0.87 g, 0.087 mmol, 1 equiv.) was added NaH (0.021 g, 0.87 mmol, 10 equiv. aimed for circa 5% allyl functional groups on dPG) and the reaction mixture was run for 1 h at room temperature. The mixture was then cooled down in an ice bath and allyl bromide (0.11 mL, 1.3 mmol, 15 equiv.) was added gradually to the mixture. The reaction was stirred overnight and subjected then to dialysis against water by using 2 kDa cut-off dialysis tube for 2 d. The purified product was concentrated and stocked as an aqueous solution (82% isolated yield).  $^1\text{H}$  NMR (500 MHz,  $\text{D}_2\text{O}$ ,  $\delta$  [ppm]): 0.91 (3H, broad s, initiator backbone), 1.40 (2H, broad s, initiator backbone), 3.34–4.20 (m, backbone repeating units), 5.27 (1H, broad s), 5.35 (1H, broad s) and 5.99 (1H, broad s) (Figure S12, Supporting Information).

**Functionalization of dPG Amine 7:** Dried dPG 4 (5 g, 0.5 mmol, 1 equiv.) was dissolved in DMF (50 mL) and to a solution of dPG was added TEA (0.9 mL, 6.5 mmol, 13 equiv.). The reaction flask was then cooled down with ice bath and methanesulfonyl chloride (0.39 mL, 5 mmol, 10 equiv. aimed for roughly 5% mesyl groups on dPG) was later added dropwise. The solution was allowed to run overnight. Afterward,  $\text{NaN}_3$  (0.65 g,

10 mmol, 20 equiv.) was added to the mixture and it was then stirred and heated up at 60 °C for 2 d. Later the crude mixture was subjected to dialysis with 2 kDa cutoff tube against water for 2 d. Then the crude product was lyophilized and collected as a viscous sticky liquid. Afterward, to the DMF (40 mL) solution of crude dPG azide was added the tetrahydrofuran (THF, 30 mL) solution of triphenylphosphine (3.28 g, 12.5 mmol, 25 equiv.) and the mixture was maintained in clear solution and stirred overnight. Later water (5 mL) was added to the solution and the mixture was allowed to stir overnight. The purification was then taken place by first washing the mixture with DCM followed by ethyl acetate, and then dialyzing the aqueous crude with 2 kDa cutoff tube against water for 2 d. The purified aqueous product was subsequently concentrated and lyophilized overnight, resulted in pale yellowish honey-like liquid (70% isolated yield). <sup>1</sup>H NMR (700 MHz, D<sub>2</sub>O, δ [ppm]): 0.90 (3H, broad s, initiator backbone), 1.39 (2H, broad s, initiator backbone), and 2.73–4.02 (m, backbone repeating units), (Figure S13, Supporting Information). <sup>13</sup>C NMR (700 MHz, D<sub>2</sub>O, δ [ppm]): 43.1 (s, 2nd CH<sub>2</sub>-NH<sub>2</sub>), 60.9–79.8 (m, polymer backbone) (Figure S14, Supporting Information).

**Quantification of an Amino Group on dPG Amine (dPG NH(Boc)):** The amino functionalized dPG can be quantified by <sup>1</sup>H NMR end-group analysis. dPG amine 7 was reacted with excess of di-*tert*-butyl dicarbonate ((Boc)<sub>2</sub>O) and then purified by dialysis against water, resulting in dPG NH(Boc), after <sup>1</sup>H NMR characterization, the integral of *tert*-butyloxycarbonyl (Boc) group was related to the integral of the dPG backbone, resulting in 4% amine functional groups. <sup>1</sup>H NMR (500 MHz, D<sub>2</sub>O, δ [ppm]): 0.86 (3H, broad s, initiator backbone), 1.42 (9H, s), 3.12–4.06 (m, backbone repeating units), (Figure S15, Supporting Information).

**Functionalization of dPG Acrylamide 8:** To a DMF (10 mL) solution of dPG amine 7 (1 g, 0.1 mmol, 1 equiv.) was added TEA (0.21 mL, 1.5 mmol, 15 equiv.) and the reaction mixture was cooled down in an ice bath. Then acryloyl chloride (0.1 mL, 1.2 mmol, 12 equiv.) was added dropwise to the reaction mixture and it was allowed to run overnight. Afterward, water 10 mL was added to the mixture and the pH was adjusted to pH 9 and it was stirred at 50 °C for 2 h. then the mixture was purified by dialysis with 2 kDa cutoff tube against water for 2 d. the dialyzed product was concentrated and collected as a pale yellowish aqueous solution (79% isolated yield). <sup>1</sup>H NMR (500 MHz, D<sub>2</sub>O, δ (ppm)): 0.7 (3H, broad s, initiator backbone), 1.19 (2H, broad s, initiator backbone), 3.17–3.89 (m, backbone repeating units), 5.61 (1H, broad s), 6.04 (1H, broad s) and 6.11 (1H, broad s) (Figure S16, Supporting Information).

**General Procedure of Encapsulation Efficiency Test:** To prepare the test with sample AC11, PEG dithiol 3 (in PBS solution, 0.7 μmol, 9.3 μL), dPG acrylate 5 (0.34 μmol, 9.2 μL), fluorescence-labeled streptavidin (in PBS solution, 3 μg, 3 μL) and PBS (16.5 μL) were mixed according to the Table 1. The mixture was left at room temperature in the dark overnight. Then 700 μL PBS was added on top of the gel and it was incubated at room temperature overnight in the dark with shaking. Afterward, the volume of an aliquot on top of the gel was measured and determined by fluorescence spectroscopy. The fluorescence intensity was then calculated to quantify the amount of streptavidin staying in the solution and the one left inside the gel. This protocol was applied to all hydrogel samples except the study of UV exposure time of gel AM2.

**Quantification of Accessible Binding Site of Encapsulated Streptavidin by HABA:** The determination of the binding site of the streptavidin encapsulated in thiol-acrylate, thiol-allyl or thiol-acrylamide hydrogels were in the same manner. To quantify the binding site of streptavidin encapsulated thiol-acrylate hydrogel (20% w/v, 38 μL, 2:1 mole ratio of PEG:dPG), PEG dithiol 3 (in PBS solution, 0.7 μmol, 9.3 μL), dPG acrylate 5 (0.34 μmol, 9.2 μL), non-labeled streptavidin (in PBS solution, 50 μg, 12.5 μL), and PBS (7 μL) were mixed. In case of thiol-allyl and thiol-acrylamide hydrogels, a mixture (with additional 10 mol% of LAP added) was subjected to 365 nm UV light for 10 min. Then all samples were placed in the dark at room temperature overnight. To each sample was subsequently added PBS (150 μL) and HABA (1 μg, 1 μL) and all samples were subsequently incubated with shaking at room temperature overnight. Afterward, the UV absorbance of HABA-streptavidin complex of each sample was measured at 500 nm.

**Quantification of Accessible Binding Site of Encapsulated Streptavidin by Biotin:** The binding site of encapsulated streptavidin of each gel type can be determined in the similar way. To quantify the binding site of streptavidin encapsulated thiol-acrylate hydrogel (20% w/v, 38 μL, 2:1 mole ratio of PEG:dPG), PEG dithiol 3 (in PBS solution, 0.7 μmol, 9.3 μL), dPG acrylate 5 (0.34 μmol, 9.2 μL), HABA-Streptavidin complex (in PBS solution, 50 μg, 12.5 μL), and PBS (7 μL) were mixed. The sample was placed in the dark overnight. PBS (150 μL) and biotin (5 μg, 5 μL) were then added to the sample and it was shaken and incubated at room temperature overnight. In the next day, the UV absorbance of biotin was measured at 350 nm.

**Calculation of the Mesh Size of a Hydrogel:** The mesh size of the thiol-acrylate (AC2), -allyl (AL1), and -acrylamide (AM1) hydrogels at 20%w/v and 2:1 mole ratio was directly calculated from the storage modulus value received from oscillatory frequency sweep test at 1 Hz shown on Figure 2. A mesh size can be calculated from the classical theory of rubber elasticity as shown below:<sup>[47,64,65]</sup>

$$r = \left( \frac{6RT}{\pi N_{AV}G} \right)^{\frac{1}{3}} \quad (1)$$

where  $r$  is mesh size (nm),  $R$  is gas constant (8.314 m<sup>3</sup>·Pa·K<sup>-1</sup>·mol<sup>-1</sup>),  $T$  is temperature (K),  $\pi$  is Pi constant (3.142),  $N_{AV}$  is Avogadro's number (6.022 × 10<sup>23</sup> mol<sup>-1</sup>), and  $G$  is storage shear modulus (Pa). The resulting mesh size is shown in Figure S7, Supporting Information.

**Preparation of an In Situ Encapsulated-Streptavidin Hydrogel for the Release Study:** The preparation of a release study is similar to the experiment of encapsulation efficiency but has differences in the period of time of incubation and the washing. All samples were prepared according to the Table 1. Thiol-allyl (AL2) and -acrylamide (AM2) gels were exposed to UV light at 365 nm for 10 min. All samples were then incubated with 600 μL PBS solution from day 1 till day 11. The aliquot was collected at day 1, 2, 3, 4, 5, 7 and 11 and each time after the fluorescence intensity of an aliquot was measured, the taken aliquot was replenished with 600 μL fresh PBS solution to the respective hydrogel sample to be incubated until the next collection time. After the calculation, the percentage of release was reported as total release as it was summed from the beginning to the end of the measurement.

**Preparation of a Hydrogel for the Degradation Study:** Thiol-acrylate (AC2), -allyl (AL1), and -acrylamide (AM1) hydrogels were prepared according to Table S2, Supporting Information. After the gel was settled overnight, the gel was removed from the mold and put to the bigger container. A 600 μL phosphate-buffered saline (PBS) solution was then put to the container and it was incubated for 11 days. The gel strength was measured at day 1, 2, 5, 7, and 11 by the rheometer with the condition mentioned earlier at 25 and 37 °C. In the case of a degradation study by NMR, gel permeation chromatography (GPC) and mass loss experiments, all the samples were prepared in the similar manner but had a difference in using deuterium PBS which was prepared by lyophilizing the normal PBS solution and then redissolving back in the same volume with D<sub>2</sub>O. The incubation was run at 37 °C for 14 days and the aliquot was collected and determined by <sup>1</sup>H NMR at day 4, 7, 9, 11, and 14. Each collected aliquot was later lyophilized and weighed to be calculated as a dry mass of a gel fragment which was found in the aliquot for mass loss experiment. The lyophilized aliquot at day 4 and day 11 of each sample was later determined by GPC.

## Supporting Information

Supporting Information is available from the Wiley Online Library or from the author.

## Acknowledgements

The authors would like to acknowledge the Core Facility BioSupraMol for the NMR measurements and Cathleen Hudziak for the help in measuring



GPC. The authors would also like to thank Matthias Wallert for providing dPG. The study was funded by Helmholtz Graduate School of Macromolecular Bioscience, Dahlem Research School of the Freie Universität Berlin and The Federal Ministry of Education and Research (BMBF).

Open access funding enabled and organized by Projekt DEAL.

## Conflict of Interest

The authors declare no conflict of interest.

## Data Availability Statement

The data that support the findings of this study are available in the supplementary material of this article.

## Keywords

3D hydrogels, encapsulation efficiency, release and degradation study, streptavidin, thiol-click chemistry

Received: July 28, 2022

Revised: September 8, 2022

Published online: October 20, 2022

- [1] A. Herrmann, R. Haag, U. Schedler, *Adv. Healthcare Mater.* **2021**, *10*, 2100062.
- [2] A. Herrmann, L. Kaufmann, P. Dey, R. Haag, U. Schedler, *ACS Appl. Mater. Interfaces* **2018**, *10*, 11382.
- [3] P. C. Weber, D. H. Ohlendorf, J. J. Wendoloski, F. R. Salemme, *Science* **1989**, *243*, 85.
- [4] S. K. Avrantinis, R. L. Stafford, X. Tian, G. A. Weiss, *ChemBioChem* **2002**, *3*, 1229.
- [5] F. Liu, J. Z. H. Zhang, Y. Mei, *Sci. Rep.* **2016**, *6*, 27190.
- [6] P. H. E. Hamming, J. Huskens, *ACS Appl. Mater. Interfaces* **2021**, *13*, 58114.
- [7] L. Välimaa, K. Pettersson, M. Vehniäinen, M. Karp, T. Lövgren, *Bioconjugate Chem.* **2003**, *14*, 103.
- [8] J. M. Alonso, A. Reichel, J. Piehler, A. del Campo, A. del Campo, *Langmuir* **2008**, *24*, 448.
- [9] R. D'Agata, P. Palladino, G. Spoto, *Beilstein J. Nanotechnol.* **2017**, *8*, 1.
- [10] S. Li, H. Liu, N. He, *J. Nanosci. Nanotechnol.* **2010**, *10*, 4875.
- [11] Y. Maeda, T. Yoshino, M. Takahashi, H. Ginya, J. Asahina, H. Tajima, T. Matsunaga, *Appl. Environ. Microbiol.* **2008**, *74*, 5139.
- [12] J. Pivetal, F. M. Pereira, A. I. Barbosa, A. P. Castanheira, N. M. Reis, A. D. Edwards, *Analyst* **2017**, *142*, 959.
- [13] A. Jo, R. Zhang, I. C. Allen, J. S. Riffle, R. M. Davis, *Langmuir* **2018**, *34*, 15783.
- [14] A. Hennig, P. M. Dietrich, F. Hemmann, T. Thiele, H. Borchering, A. Hoffmann, U. Schedler, C. Jäger, U. Resch-Genger, W. E. S. Unger, *Analyst* **2015**, *140*, 1804.
- [15] M.-Y. Hong, Y.-J. Kim, J. W. Lee, K. Kim, J.-H. Lee, J.-S. Yoo, S.-H. Bae, B.-S. Choi, H.-S. Kim, *J. Colloid Interface Sci.* **2004**, *274*, 41.
- [16] P. Dey, M. Adamovski, S. Friebe, A. Badalyan, R.-C. Mutihac, F. Paulus, S. Leimkühler, U. Wollenberger, R. Haag, *ACS Appl. Mater. Interfaces* **2014**, *6*, 8937.
- [17] K. Awsyuk, P. Petrou, A. Thanassoulas, J. Raczowska, *Langmuir* **2019**, *35*, 3058.
- [18] X. Duan, Y. Li, N. K. Rajan, D. A. Routenberg, Y. Modis, M. A. Reed, *Nat. Nanotechnol.* **2012**, *7*, 401.
- [19] F. Reisbeck, S. Wedepohl, M. Dimde, A.-C. Schmitt, J. Dervede, M. Álvaro-Benito, C. Freund, R. Haag, *J. Mater. Chem. B* **2021**, *10*, 96.
- [20] R. Randriantsilefisoa, J. L. Cuellar-Camacho, M. S. Chowdhury, P. Dey, U. Schedler, R. Haag, *J. Mater. Chem. B* **2019**, *7*, 3220.
- [21] W. Liang, S. Bhatia, F. Reisbeck, Y. Zhong, A. K. Singh, W. Li, R. Haag, *Adv. Funct. Mater.* **2021**, *31*, 2010630.
- [22] C. E. Ziegler, M. Graf, M. Nagaoka, H. Lehr, A. M. Goepferich, *Biomacromolecules* **2021**, *22*, 3223.
- [23] A. Oehrl, S. Schötz, R. Haag, *Macromol. Rapid Commun.* **2020**, *41*, 1900510.
- [24] J. J. Roberts, S. J. Bryant, *Biomaterials* **2013**, *34*, 9969.
- [25] A. A. Aimetti, A. J. Machen, K. S. Anseth, *Biomaterials* **2009**, *30*, 6048.
- [26] C. E. Hoyle, A. B. Lowe, C. N. Bowman, *Chem. Soc. Rev.* **2010**, *39*, 1355.
- [27] C. E. Hoyle, C. N. Bowman, *Angew. Chem., Int. Ed.* **2010**, *49*, 1540.
- [28] S. H. Mahadevegowda, M. C. Stuparu, *Eur. J. Org. Chem.* **2017**, *2017*, 570.
- [29] S. Roller, H. Zhou, R. Haag, *Mol. Diversity* **2005**, *9*, 305.
- [30] D. L. Elbert, J. A. Hubbell, *Biomacromolecules* **2001**, *2*, 430.
- [31] N. Hammer, F. P. Brandl, S. Kirchhof, V. Messmann, A. M. Goepferich, *Macromol. Biosci.* **2015**, *15*, 405.
- [32] R. C. Laible, *Chem. Rev.* **1958**, *58*, 807.
- [33] S. J. Oh, D. R. Kinney, W. Wang, P. L. Rinaldi, *Macromolecules* **2002**, *35*, 2602.
- [34] M. B. Larsen, S.-J. Wang, M. A. Hillmyer, *J. Am. Chem. Soc.* **2018**, *140*, 11911.
- [35] F. Dénès, M. Pichowicz, G. Povie, P. Renaud, *Chem. Rev.* **2014**, *114*, 2587.
- [36] I. Degirmenci, M. L. Coote, *J. Phys. Chem. A* **2016**, *120*, 1750.
- [37] M. A. Blot, *Appl. Sci. Res., Sect. A* **1963**, *12*, 168.
- [38] V. Trujillo, J. Kim, R. C. Hayward, *Soft Matter* **2008**, *4*, 564.
- [39] D. Bermejo-Velasco, A. Azémar, O. P. Oommen, J. Hilborn, O. P. Varghese, *Biomacromolecules* **2019**, *20*, 1412.
- [40] I. M. Kolthoff, W. Stricks, R. C. Kapoor, *J. Am. Chem. Soc.* **1955**, *77*, 4733.
- [41] D. P. Nair, M. Podgórski, S. Chatani, T. Gong, W. Xi, C. R. Fenoli, C. N. Bowman, *Chem. Mater.* **2014**, *26*, 724.
- [42] A. K. Nguyen, P. L. Goering, V. Reipa, R. J. Narayan, *Biointerphases* **2019**, *14*, 021007.
- [43] J. S. Ribeiro, A. Dagherry, N. Dubey, C. Li, L. Mei, J. C. Fenno, A. Schwendeman, Z. Aytac, M. C. Bottino, *Biomacromolecules* **2020**, *21*, 3945.
- [44] J. D. Mccall, K. S. Anseth, *Biomacromolecules* **2012**, *13*, 2410.
- [45] M. Porel, J. S. Brown, C. A. Alabi, *Synlett* **2015**, *26*, 565.
- [46] J. S. Brown, A. W. Ruttinger, A. J. Vaidya, C. A. Alabi, P. Clancy, *Org. Biomol. Chem.* **2020**, *18*, 6364.
- [47] J. Li, D. J. Mooney, *Nat. Rev. Mater.* **2016**, *1*, 16071.
- [48] T. Shirakura, T. J. Kelson, A. Ray, A. E. Malyarenko, R. Kopelman, *ACS Macro Lett.* **2014**, *3*, 602.
- [49] G. W. Ashley, J. Henise, R. Reid, D. V. Santi, *Proc. Natl. Acad. Sci. USA* **2013**, *110*, 2318.
- [50] A. Puiggalf-Jou, E. Cazorla, G. Ruano, I. Babeli, M.-P. Ginebra, J. García-Torres, C. Alemán, *ACS Biomater. Sci. Eng.* **2020**, *6*, 6228.
- [51] S. Sheth, E. Barnard, B. Hyatt, M. Rathinam, S. P. Zusiak, *Front. Bioeng. Biotechnol.* **2019**, *7*, 410.
- [52] X. Tong, J. Lai, B.-H. Guo, Y. Huang, *J. Polym. Sci., Part A: Polym. Chem.* **2011**, *49*, 1513.
- [53] A. Metters, J. Hubbell, *Biomacromolecules* **2005**, *6*, 290.
- [54] J. P. Wagner, P. R. Schreiner, *Angew. Chem., Int. Ed.* **2015**, *54*, 12274.
- [55] D. Shao, K. Tapio, S. Auer, J. J. Toppari, V. P. Hytönen, M. Ahlskog, *Langmuir* **2018**, *34*, 15335.

- [56] I. Le Trong, N. Humbert, T. R. Ward, R. E. Stenkamp, *J. Mol. Biol.* **2006**, 356, 738.
- [57] Q. Xu, L. Guo, S. A. Y. Gao, D. Zhou, U. Greiser, J. Creagh-Flynn, H. Zhang, Y. Dong, L. Cutlar, F. Wang, W. Liu, W. Wang, W. Wang, *Chem. Sci.* **2018**, 9, 2179.
- [58] X. Li, S. A. Q. Xu, F. Alshehri, M. Zeng, D. Zhou, J. Li, G. Zhou, W. Wang, *ACS Appl. Bio Mater.* **2020**, 3, 4756.
- [59] S. Stichler, T. Jungst, M. Schamel, I. Zilkowski, M. Kuhlmann, T. Böck, T. Blunk, J. Teßmar, J. Groll, *Ann. Biomed. Eng.* **2017**, 45, 273.
- [60] R. Haag, A. Sunder, J.-F. Stumbé, *Angew. Chem., Int. Ed* **1996**, 38, 17.
- [61] A. Sunder, R. Hanselmann, H. Frey, R. Mülhaupt, *Macromolecules* **1999**, 32, 4240.
- [62] H. Frey, R. Haag, *Rev. Mol. Biotechnol.* **2002**, 90, 257.
- [63] M. Wallert, J. Plaschke, M. Dimde, V. Ahmadi, S. Block, R. Haag, *Macromol. Mater. Eng.* **2021**, 306, 2000688.
- [64] A. J. Kuijpers, G. H. M. Engbers, J. Feijen, S. C. De Smedt, T. K. L. Meyvis, J. Demeester, J. Krijgsveld, S. A. J. Zaat, J. Dankert, *Macromolecules* **1999**, 32, 3325.
- [65] K. S. Anseth, C. N. Bowman, L. Brannon-Peppas, *Biomaterials* **1996**, 17, 1647.